Journal of Probability and Statistical Science
24(2), 1-15Aug. 2026

A Flexible Heavy-Tailed Distribution via the Modified Kies Family: Theory and Applications

Ehinomen Emmanuel Ehizojie
Department of Statistics, Faculty of Physical Sciences
Ahmadu Bello University, Zaria Nigeria.

ABSTRACT

This paper introduces a new heavy-tailed distribution as an alternative to the classical Inverse Lomax distribution, constructed through the Modified Kies generator. The proposed Modified Kies Inverse Lomax distribution (MKILD) is designed to model real lifetime data characterised by skewness, high kurtosis, and the presence of outlying observations. Its density function exhibits considerable flexibility, accommodating decreasing, nearly symmetric, and left- or right-skewed unimodal shapes, while its hazard rate captures both increasing and decreasing patterns. Several statistical properties are derived, including order statistics, quantile function, moments, probability weighted moments, skewness, and kurtosis. Parameter estimation is carried out using six methods: maximum likelihood, maximum product of spacing, Anderson-Darling, Cramér-von Mises, least squares, and weighted least squares. Simulation studies confirm that biases and mean squared errors diminish consistently with increasing sample size, with maximum likelihood proving the most efficient across most settings. Three real-life applications to lifetime datasets establish that the MKILD provides a competitive fit compared to the classical ILD and several of its generalisations, namely the Power ILD, Marshall-Olkin ILD, Exponentiated Generalised ILD, and Odd Fréchet ILD.

Keywords: Modified Kies family, Inverse Lomax distribution, Heavy-tailed distribution, Estimations, Goodness-of-fit

1. Introduction

The Selection of an appropriate probability model for observed phenomena remains a fundamental challenge in statistical science, one deeply rooted in probability distribution theory. This theory provides a rigorous mathematical language for characterising uncertainty, enabling researchers to quantify the likelihood of various outcomes and to capture the stochastic mechanisms that generate data. A probability distribution, whether expressed through its cumulative distribution function (CDF), probability density function (PDF), or hazard rate function, serves as a theoretical description of observed data patterns. Nevertheless, many practical datasets exhibit features such as heavy tails, skewness, multiple modes, or non-monotonic hazard rates that classical distributions are ill-equipped to handle. This reality has driven a sustained effort in modern statistics towards developing flexible extensions and generalisations of baseline models, particularly those capable of accommodating heavy-tailed behaviour across survival analysis, reliability engineering, actuarial science, and environmental studies.

The Lomax distribution, also referred to as the Pareto type II distribution and introduced by Lomax (1954), is a special case of the generalised Pareto distribution and arises in numerous applied settings, including actuarial science, economics, income and wealth data, modelling business failure times, biological sciences, firm size studies, queuing problems, reliability modelling, and life testing (Harris, 1968; Atkinson and Harrison, 1978; Holland *et al.*, 2006;

- Received May 21, 2026, in final form August 2026.
- Ehinomen Emmanuel Ehizojie (corresponding author) is affiliated with Department of Statistics, Ahmadu Bello University, Zaria, Nigeria.
  Email:ehizojieee@gmail.com

Hassan and Al-Ghamdi, 2009; Corbellini *et al.*, 2010; Al-Zahrani and Al-Sobhi, 2013; Hassan *et al.*, 2016).

Among the notable members of the Lomax family is the Inverse Lomax distribution (ILD), which arises as a special case of the generalised beta distribution of the second kind. The ILD has attracted considerable attention owing to its capacity for modelling heavy-tailed lifetime data, particularly in datasets where high failure rates occur during the early stages of operation. Its usefulness spans several applied domains, including economics and actuarial science, where it describes size distributions and associated tail risks, and geophysics, where it has supported the analysis of extreme values such as land fibre sizes (Kleiber and Kotz, 2003; Al-Marzouki *et al.*, 2021). Its mathematical and inferential properties have been studied extensively by Rahman *et al.* (2013), Yadav *et al.* (2016), and Yadav *et al.* (2019), further cementing its role as a tractable model for data with heavy-tailed characteristics.

The practical usefulness of the ILD has motivated the development of numerous generalisations and modified variants aimed at improving its flexibility and modelling performance. Existing extensions include the Weibull ILD (Hassan and Mohamed, 2019), Marshall-Olkin ILD (Maxwell *et al.*, 2019), Discrete Alpha Power ILD (Almetwally and Ibrahim, 2020), Alpha Power Transformed ILD (ZeinEldin *et al.*, 2020a), Odd Fréchet ILD (ZeinEldin *et al.*, 2020b), Modified Logarithmic Transformed ILD (Almarashi, 2021), Half Logistic ILD (Al-Marzouki *et al.*, 2021), Kumaraswamy Generalised ILD (Ogunde *et al.*, 2023), Transmuted Topp-Leone ILD (Alyami *et al.*, 2023), Type I Half Logistic Topp-Leone ILD (Adepoju *et al.*, 2024), Extended ILD (Hadi *et al.*, 2025), and Exponentiated Kumaraswamy ILD (Afere *et al.*, 2026), among others. Collectively, these studies highlight the importance of the ILD as a useful baseline model for constructing more flexible lifetime distributions.

Despite these developments, several existing generalisations of the ILD still exhibit important limitations. Some models require the introduction of multiple additional parameters, resulting in increased model complexity, parameter identifiability challenges, and computational difficulties during estimation procedures. In some cases, the resulting hazard rate structures remain insufficiently flexible for modelling diverse reliability behaviours observed in practice. Other extensions may provide improved tail behaviour but lack analytical tractability, thereby complicating statistical inference and practical implementation under censored or complete sampling schemes. Furthermore, certain generated ILDs may fail to simultaneously accommodate varying degrees of skewness, kurtosis, and complex hazard rate patterns within a relatively parsimonious structure. These limitations continue to motivate the search for more flexible and computationally efficient extensions of the ILD.

In recent years, generator-based distribution families have emerged as effective approaches for enhancing the flexibility of baseline distributions. Among these, the Modified Kies (MKi) family introduced by Al-Babtain *et al.* (2020) has gained considerable attention because of its attractive statistical and analytical properties. The family was developed using the generator approach of Alzaatreh *et al.* (2013) and is capable of producing density functions with varying degrees of skewness and tail behaviour whilst accommodating increasing, decreasing, and bathtub-shaped hazard rate functions. Such flexibility is particularly important in survival and reliability analysis where lifetime data frequently exhibit non-monotonic failure mechanisms.

In the context of extending the ILD, the MKi generator offers several specific benefits. First, because the MKi CDF takes a closed form, the resulting model retains analytical tractability, facilitating mathematical derivations, enabling straightforward maximum likelihood

estimation under both complete and right-censored samples. Second, the generator introduces a single additional shape parameter that directly controls the tail behaviour and hazard rate shape, thereby improving flexibility without inducing over-parameterisation. Third, the transformation involved in the MKi family tends to produce a more pronounced capability for modelling early failure phases and heavy tails simultaneously, a feature often lacking in simpler generalisations of the ILD. These attributes collectively make the MKi generator a compelling tool for constructing a novel lifetime distribution based on the ILD.

Motivated by the aforementioned limitations and advantages, this study proposes a new extension of the ILD based on the MKi generator. The proposed model seeks to improve the flexibility of the classical ILD by providing greater adaptability in modelling skewed and heavy-tailed lifetime data with diverse hazard rate behaviours. The resulting distribution is expected to offer enhanced fitting performance, analytical tractability, and broader applicability in reliability, survival, engineering, and actuarial studies.

Considering the ILD with shape parameter $\alpha > 0$ and scale parameter $\beta > 0$, the CDF and PDF are respectively given by

$$G(x;\alpha,\beta) = \left(1+\frac{\beta}{x}\right)^{-\alpha}; \qquad x \in \mathbb{R}^+, \tag{1}$$

and

$$g(x;\alpha,\beta) = \alpha\beta x^{-2}\left(1+\frac{\beta}{x}\right)^{-\alpha-1}. \tag{2}$$

The CDF and PDF of the MKi family with a shape parameter $\lambda > 0$ (for $x \in \mathbb{R}^+$) respectively defined as

$$F(x;\lambda) = 1 - \exp\left[-\left(\frac{G(x)}{1-G(x)}\right)^{\lambda}\right], \tag{3}$$

and

$$f(x;\lambda) = \lambda\frac{g(x)G(x)^{\lambda-1}}{\left(1-G(x)\right)^{\lambda+1}}\exp\left[-\left(\frac{G(x)}{1-G(x)}\right)^{\lambda}\right], \tag{4}$$

where $G(x)$ and $g(x)$ denote the baseline CDF and PDF, respectively.

2. Formulation of the Proposed Model

Let X be a non-negative random variable following the modified Kies inverse Lomax distribution. Using the MKi generator defined in Equations (3) and (4) with the ILD's CDF and PDF respectively given Equations (1) and (2), thus, the CDF and PDF are respectively given by

$$F(x;\alpha,\beta,\lambda) = 1 - \exp\left[-\left(\frac{\left(1+\frac{\beta}{x}\right)^{-\alpha}}{1-\left(1+\frac{\beta}{x}\right)^{-\alpha}}\right)^{\lambda}\right], \qquad x,\alpha,\beta,\lambda > 0, \tag{5}$$

and

$$f(x;\alpha,\beta,\lambda)=\frac{\alpha\beta\lambda x^{-2}\left(1+\frac{\beta}{x}\right)^{-\alpha\lambda-1}}{\left(1-\left(1+\frac{\beta}{x}\right)^{-\alpha}\right)^{\lambda+1}}\exp\left[-\left(\frac{\left(1+\frac{\beta}{x}\right)^{-\alpha}}{1-\left(1+\frac{\beta}{x}\right)^{-\alpha}}\right)^{\lambda}\right], \quad (6)$$

where β is the scale parameter; α and λ are the shape parameters, respectively.

The graphical representation of the PDF of the MKILD is illustrated in Figure 1. It is seen that the density of MKILD exhibits decreasing, closely symmetric, left-skewed or right-skewed unimodal shapes for some selected parameter values of the distribution.

Figure 1 displays the PDF of the MKILD for selected parameter values. The density exhibits a range of shapes, including strictly decreasing, nearly symmetric unimodal, left-skewed unimodal, and right-skewed unimodal forms. This flexibility indicates the suitability of the MKILD for modelling heterogeneous lifetime and reliability data.

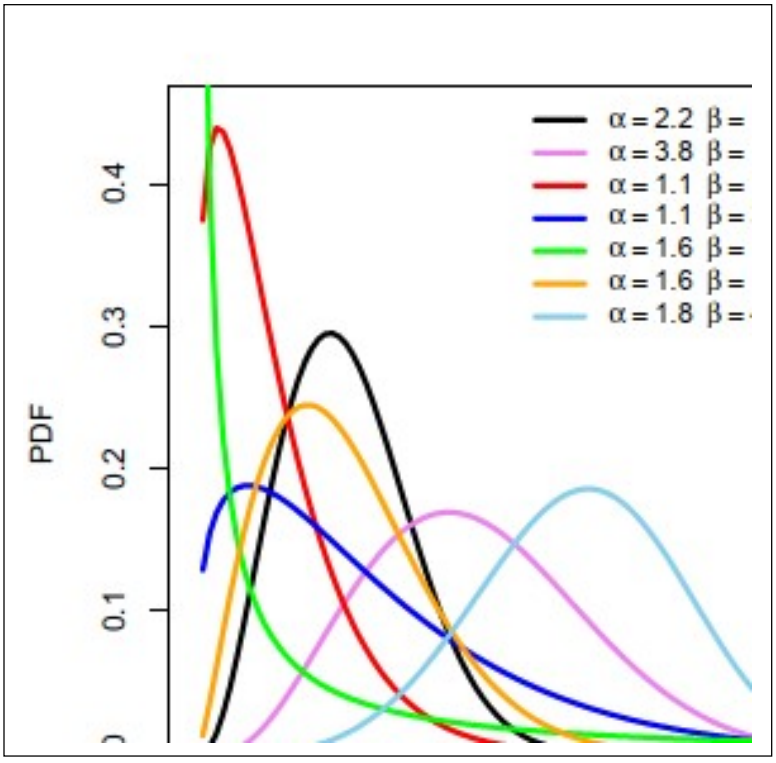


Figure 1: The PDF plot of the MKILD.

3. Statistical Properties

In this section, some important characteristics of the MKILD are investigated.

3.1 Series Representations for the CDF and PDF

For mathematical tractability, particularly for deriving moments, quantile functions, and entropy measures, it is convenient to express the CDF and PDF as infinite series. The exponential series expansion is derived as follows

letting $z=\left(1+\frac{\beta}{x}\right)^{-\alpha}$ then Equation (5) becomes

$$F(x) = 1 - \exp\left[-\left(\frac{z}{1-z}\right)^{\lambda}\right].$$

Using the exponential series expansion

$$e^{-u} = \sum_{i=0}^{\infty} \frac{(-1)^i u^i}{i!},$$

yields

$$F(x) = 1 - \sum_{i=0}^{\infty} \frac{(-1)^i}{i!}\left(\frac{z}{1-z}\right)^{\lambda i}.$$

Hence,

$$F(x) = \sum_{i=1}^{\infty} \frac{(-1)^{i+1}}{i!} z^{\lambda i}(1-z)^{-\lambda i}.$$

Applying the generalised binomial expansion

$$(1-z)^{-a} = \sum_{j=0}^{\infty} \frac{\Gamma(a+j)}{\Gamma(a)\Gamma(j+1)} z^j, \quad |z| < 1,$$

yields

$$F(x) = \sum_{i=1}^{\infty}\sum_{j=0}^{\infty} \frac{(-1)^{i+1}}{i!} \frac{\Gamma(\lambda i + j)}{\Gamma(\lambda i)\Gamma(j+1)} z^{\lambda i + j}.$$

The series representation of the CDF becomes

$$F(x) = \sum_{i=1}^{\infty}\sum_{j=0}^{\infty} \frac{(-1)^{i+1}}{i!} \frac{\Gamma(\lambda i + j)}{\Gamma(\lambda i)\Gamma(j+1)} \left(1 + \frac{\beta}{x}\right)^{-\alpha(\lambda i + j)}. \tag{7}$$

Similarly, the series representation of the PDF is obtained as follows:

letting $z = \left(1 + \frac{\beta}{x}\right)^{-\alpha}$ then Equation (6) becomes

$$f(x) = \alpha\beta\lambda x^{-2}\left(1 + \frac{\beta}{x}\right)^{-\alpha\lambda - 1}(1-z)^{-(\lambda+1)} \exp\left[-\left(\frac{z}{1-z}\right)^{\lambda}\right],$$

Using the exponential expansion,

$$\exp\left[-\left(\frac{z}{1-z}\right)^{\lambda}\right] = \sum_{i=0}^{\infty} \frac{(-1)^i}{i!} z^{\lambda i}(1-z)^{-\lambda i},$$

gives

$$f(x) = \alpha\beta\lambda x^{-2}\left(1+\frac{\beta}{x}\right)^{-\alpha\lambda-1}\sum_{i=0}^{\infty}\frac{(-1)^i}{i!}z^{\lambda i}(1-z)^{-(\lambda i+\lambda+1)}.$$

Again, applying the generalised binomial expansion,

$$(1-z)^{-(\lambda i+\lambda+1)} = \sum_{j=0}^{\infty}\frac{\Gamma(\lambda i+\lambda+j+1)}{\Gamma(\lambda i+\lambda+1)\Gamma(j+1)}z^j,$$

yields

$$f(x) = \alpha\beta\lambda x^{-2}\left(1+\frac{\beta}{x}\right)^{-\alpha\lambda-1}\sum_{i=0}^{\infty}\sum_{j=0}^{\infty}\frac{(-1)^i}{i!}\frac{\Gamma(\lambda i+\lambda+j+1)}{\Gamma(\lambda i+\lambda+1)\Gamma(j+1)}z^{\lambda i+j}.$$

Thus, the PDF admits the following series representation

$$f(x) = \sum_{i=0}^{\infty}\sum_{j=0}^{\infty}w_{i,j}\,x^{-2}\left(1+\frac{\beta}{x}\right)^{-\alpha(\lambda i+j+\lambda)-1} \tag{8}$$

where

$$w_{i,j} = \frac{\alpha\beta\lambda(-1)^i}{i!}\frac{\Gamma(\lambda i+\lambda+j+1)}{\Gamma(\lambda i+\lambda+1)\Gamma(j+1)}.$$

Equations (7) and (8) provide useful linear representations of the CDF and PDF of the MKILD, which facilitate the derivation of several structural properties such as moments, order statistics, reliability measures, and entropy characteristics.

3.2 Ordinary Moments

The ordinary rth moment of the MKILD is defined as

$$\mu'_r = E(X^r) = \int_0^{\infty}x^r f(x)dx. \tag{9}$$

Substituting the series representation of the PDF given in Equation (8), into Equation (9), yields

$$\mu'_r = \sum_{i=0}^{\infty}\sum_{j=0}^{\infty}w_{i,j}\int_0^{\infty}x^{r-2}\left(1+\frac{\beta}{x}\right)^{-\alpha(\lambda i+j+\lambda)-1}dx,$$

letting $c_{i,j} = \alpha(\lambda i+j+\lambda)+1$, then,

$$\mu'_r = \sum_{i=0}^{\infty}\sum_{j=0}^{\infty}w_{i,j}\int_0^{\infty}x^{r-2}\left(1+\frac{\beta}{x}\right)^{-c_{i,j}}dx. \tag{10}$$

Now observe that

$$\left(1+\frac{\beta}{x}\right)^{-c_{i,j}} = \left(\frac{x}{x+\beta}\right)^{c_{i,j}} = x^{c_{i,j}}(x+\beta)^{-c_{i,j}}.$$

Hence,

$$\mu_r' = \sum_{i=0}^{\infty}\sum_{j=0}^{\infty} w_{i,j} \int_0^{\infty} x^{r+c_{i,j}-2} (x+\beta)^{-c_{i,j}} dx.$$

Using the transformation: $x = \beta u, \quad dx = \beta du$,gives

$$\mu_r' = \sum_{i=0}^{\infty}\sum_{j=0}^{\infty} w_{i,j}\, \beta^r \int_0^{\infty} u^{r+c_{i,j}-2} (1+u)^{-c_{i,j}} du.$$

Applying the Beta function identity

$$\int_0^{\infty} u^{m-1} (1+u)^{-n} du = B(m, n-m) = \frac{\Gamma(m)\Gamma(n-m)}{\Gamma(n)},$$

where $n > m > 0$, setting $m = r + c_{i,j} - 1, \quad n = c_{i,j}$, to obtain

$$\mu_r' = \sum_{i=0}^{\infty}\sum_{j=0}^{\infty} w_{i,j}\, \beta^r B(r + c_{i,j} - 1, 1-r).$$

$$\mu_r' = \sum_{i=0}^{\infty}\sum_{j=0}^{\infty} w_{i,j}\, \beta^r \frac{\Gamma(r + c_{i,j} - 1)\Gamma(1-r)}{\Gamma(c_{i,j})}, \quad r < 1, \tag{11}$$

where $c_{i,j} = \alpha(\lambda i + j + \lambda) + 1$, and $w_{i,j} = \frac{\alpha\beta\lambda(-1)^i}{i!} \frac{\Gamma(\lambda i+\lambda+j+1)}{\Gamma(\lambda i+\lambda+1)\Gamma(j+1)}$.

Equation (11) provides a general expression for the ordinary moments of the MKILD. Consequently, the existence of the moments depends on the condition $r < 1$, which reflects the heavy-tailed nature of the distribution.

3.3 Probability Weighted Moments

Probability weighted moments (PWMs) provide an important alternative to conventional ordinary moments, for describing its distributional characteristics. The PVMs of a random variable X are defined as

$$\tau_{r,s} = E[X^r F(X)^s] = \int_0^{\infty} x^r\, F(x)^s f(x) dx \tag{12}$$

where r and s are non-negative real numbers. For the PVM of MKILD, substituting the series representations of the MKILD given in (7) and (8) into (12), yields

$$\tau_{r,s} = \int_0^{\infty} x^r \left[\sum_{k,m} a_{k,m} \left(1 + \frac{\beta}{x}\right)^{-\alpha(\lambda k+m)}\right]^s \left[\sum_{i,j} w_{i,j}\, x^{-2} \left(1 + \frac{\beta}{x}\right)^{-\alpha(\lambda i+j+\lambda)-1}\right] dx$$

Using multinomial expansion,

$$F(x)^s = \sum_{K} A_K \left(1 + \frac{\beta}{x}\right)^{-\alpha B_K},$$

where A_K are combinatorial coefficients depending on s, and B_K is a linear combination of indices from the expansion. The PWM becomes a triple-series integral of

$$\tau_{r,s} = \sum_{i,j,K} C_{i,j,K} \int_0^\infty x^{r-2} \left(1 + \frac{\beta}{x}\right)^{-\alpha(\lambda i + j + \lambda) - 1 - \alpha B_K} dx.$$

Defining $D_{i,j,K} = \alpha(\lambda i + j + \lambda + B_K) + 1$, then,

$$\tau_{r,s} = \sum_{i,j,K} C_{i,j,K} \int_0^\infty x^{r-2} \left(1 + \frac{\beta}{x}\right)^{-D_{i,j,K}} dx.$$

$$\tau_{r,s} = \sum_{i,j,K} C_{i,j,K} \int_0^\infty x^{r+D_{i,j,K}-2} (x + \beta)^{-D_{i,j,K}} dx$$

letting $x = \beta u, \quad dx = \beta du,$ then,

$$\tau_{r,s} = \sum_{i,j,K} C_{i,j,K}\, \beta^r \int_0^\infty u^{r+D_{i,j,K}-2} (1 + u)^{-D_{i,j,K}} du$$

Using:

$$\int_0^\infty u^{m-1} (1 + u)^{-n} du = B(m, n - m),$$

yields

$$\tau_{r,s} = \sum_{i,j,K} C_{i,j,K}\, \beta^r B\left(r + D_{i,j,K} - 1, 1 - r\right).$$

Therefore, the PWM of MKILD can be expressed as

$$\tau_{r,s} = \sum_{i=0}^{\infty} \sum_{j=0}^{\infty} \sum_{K} C_{i,j,K}\, \beta^r \frac{\Gamma\left(r + D_{i,j,K} - 1\right)\Gamma(1 - r)}{\Gamma\left(D_{i,j,K}\right)}, \qquad r < 1. \tag{13}$$

3.4 Quantile Function

The quantile function (QF) can be obtained by solving $F(x) = u, \quad 0 < u < 1$. Using the CDF given in Equation (5), the QF of the MKILD is derived as follows

$$1 - \exp\left[-\left(\frac{\left(1 + \frac{\beta}{x}\right)^{-\alpha}}{1 - \left(1 + \frac{\beta}{x}\right)^{-\alpha}}\right)^{\lambda}\right] = u$$

$$\left[\frac{\left(1 + \frac{\beta}{x}\right)^{-\alpha}}{1 - \left(1 + \frac{\beta}{x}\right)^{-\alpha}}\right]^{\lambda} = -\log(1 - u)$$

$$\frac{\left(1+\frac{\beta}{x}\right)^{-\alpha}}{1-\left(1+\frac{\beta}{x}\right)^{-\alpha}} = [-\log(1-u)]^{1/\lambda}$$

$$\left(1+\frac{\beta}{x}\right)^{-\alpha} = \frac{[-\log(1-u)]^{1/\lambda}}{1+[-\log(1-u)]^{1/\lambda}}$$

$$1+\beta/x = \left[\frac{[-\log(1-u)]^{1/\lambda}}{1+[-\log(1-u)]^{1/\lambda}}\right]^{1/\alpha}$$

$$Q(u) = x_u = \frac{\beta}{\left[\frac{[-\log(1-u)]^{1/\lambda}}{1+[-\log(1-u)]^{1/\lambda}}\right]^{1/\alpha} - 1} \tag{14}$$

The QF of the MKILD is given in Equation (14). The QF enables random variate generation and facilitates the computation of quantile-based descriptive measures such as median, interquartile range, skewness and kurtosis.

3.5 Quantile-Based Skewness and Kurtosis

Since the MKILD does not possess finite ordinary moments of order greater than or equal to one, quantile-based measures provide more reliable alternatives for describing asymmetry and tail behaviour. The Bowley quantile coefficient of skewness (Bowley, 1926) is defined as

$$S_B = \frac{Q(0.75) + Q(0.25) - 2Q(0.50)}{Q(0.75) - Q(0.25)} \tag{15}$$

where $Q(\cdot)$denotes the quantile function of the MKILD.

Similarly, the Moors quantile coefficient of kurtosis (Moors, 1988) is defined as

$$K_M = \frac{Q(0.875) - Q(0.625) + Q(0.375) - Q(0.125)}{Q(0.75) - Q(0.25)} \tag{16}$$

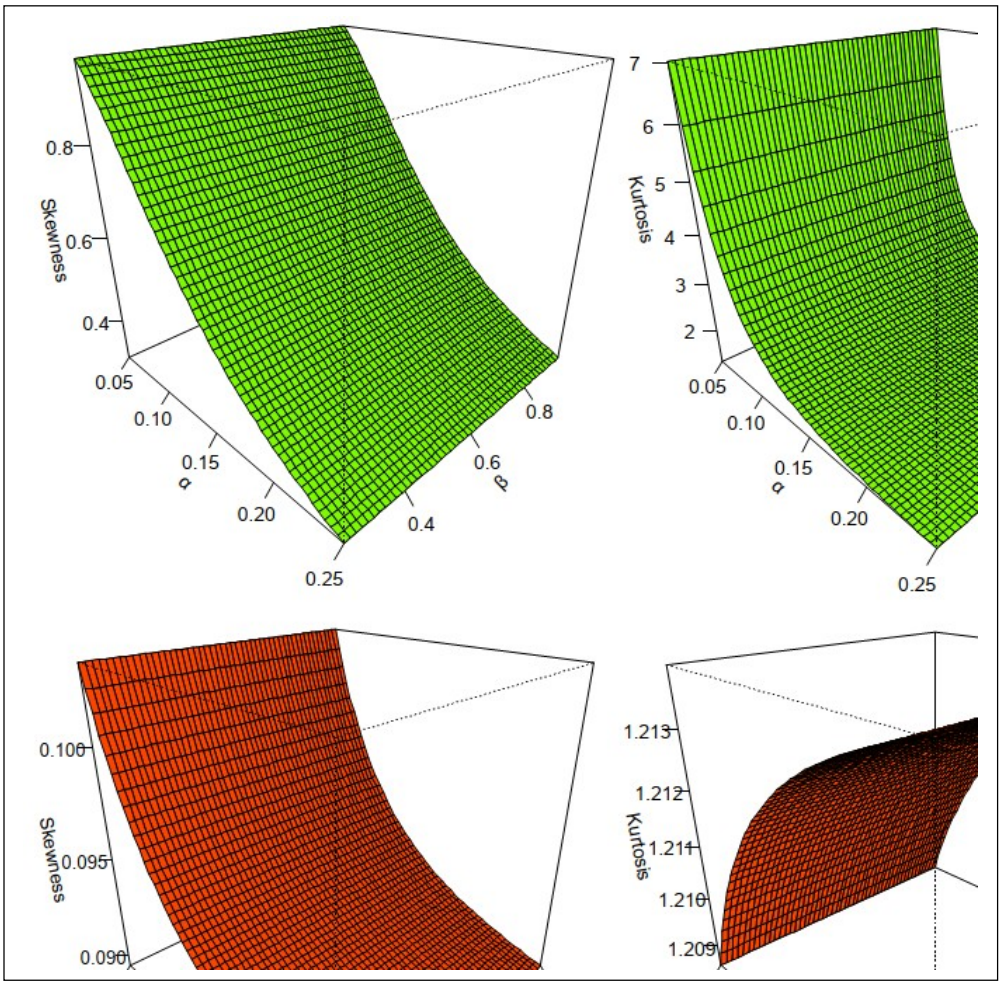
These quantile-based measures are robust against extreme observations and remain well-defined even when conventional moment-based skewness and kurtosis do not exist. Consequently, they are particularly appropriate for assessing the shape characteristics and tail heaviness of the MKILD. The numerical computation of the quartiles, octiles, Bowley's skewness and Moors' kurtosis measures of the MKILD for different values of parameters is presented in Table 1.

Table 1: Quartiles, Octiles, Bowley's skewness and Moors' kurtosis measures of the MKILD.

Parmeter → **Statistic ↓**	**(α=0.15, β=0.75, λ=1.55)**	**(α=0.35, β=0.75, λ=1.55)**	**(α=0.25, β=0.35, λ=1.75)**	**(α=0.25, β=0.65, λ=1.75)**	**(α=1.65, β=2.45, λ=0.15)**	**(α=1.65, β=2.45, λ=1.85)**	**(α=1.95, β=2.25, λ=4.05)**
Q_1 (0.25)	0.00030	0.02717	0.00416	0.00772	0.01606	2.63235	4.06651
Median (0.50)	0.00322	0.08011	0.01467	0.02724	0.67598	3.94474	4.87964
Q_3 (0.75)	0.01464	0.16862	0.03429	0.06367	36.4475	5.49071	5.65020
O_1 (0.125)	0.00003	0.00932	0.00117	0.00218	0.00072	1.87596	3.48061
O_3 (0.375)	0.00120	0.05067	0.00862	0.01601	0.12122	3.29216	4.49972
O_5 (0.625)	0.00715	0.11762	0.02279	0.04232	4.18951	4.64945	5.24979
O_7 (0.875)	0.03087	0.25056	0.05336	0.09910	533.264	6.69220	6.16329

S_B	0.59312	0.25148	0.30231	0.30231	0.96377	0.08172	-0.02689
K_M	1.73537	1.23215	1.26206	1.26206	14.5258	1.21011	1.22033

Figure 2 presents the Bowley's skewness and Moors' kurtosis plots of the MKILD for fixed $\lambda = 1.75$ for both scenarios, but $\alpha \in (0.05,0.25)$, and $\beta \in (0.25, 0.95)$ (top panel); and varying$\alpha \in (1, 2.5), \beta \in (1, 5)$ (bottom panel). It is observed that the skewness plots indicate that the distribution is predominantly right-skewed at fixed $\lambda = 1.75$, across the varying values



of α and β. The kurtosis at fixed $\lambda = 1.75$, for $\alpha \in (1, 2.5)$, and $\beta \in (1, 5)$ is a platykurtic distribution, while the distribution is mostly leptokurtic for fixed $\lambda = 1.75$ for $\alpha \in (0.05, 0.25)$, and $\beta \in (0.25, 0.95)$.

Figure 2: The skewness and kurtosis plots of the MKILD.

3.6 Reliability Analysis

Three fundamental functions in survival and reliability analysis are investigated. The survival function (SF), denoted $S(x)$, gives the probability that a unit survives beyond time x, that is, $S(x) = 1 - F(x)$. The hazard function (HF), denoted $h(x)$, represents the instantaneous failure rate at time x conditional on survival up to that time; it is defined as $h(x) = f(x)/S(x)$. The cumulative hazard function (CHF), denoted $H(x)$, is the integral of the hazard function from 0 to x and satisfies $H(x) = -\ln[1 - F(x)]$. These three functions provide

equivalent characterisations of a lifetime distribution and are particularly informative in reliability, medical survival analysis, and actuarial science.

For the MKILD with CDF and PDF given in Equations (5) and (6), the SF, HF, and CHF are respectively given as follows

$$S(x;\alpha,\beta,\lambda) = \exp\left[-\left(\frac{\left(1+\frac{\beta}{x}\right)^{-\alpha}}{1-\left(1+\frac{\beta}{x}\right)^{-\alpha}}\right)^{\lambda}\right], \tag{17}$$

$$h(x;\alpha,\beta,\lambda) = \frac{\alpha\beta\lambda x^{-2}\left(1+\frac{\beta}{x}\right)^{-\alpha\lambda-1}}{\left(1-\left(1+\frac{\beta}{x}\right)^{-\alpha}\right)^{\lambda+1}}, \tag{18}$$

and

$$H(x;\alpha,\beta,\lambda) = \left(\frac{\left(1+\frac{\beta}{x}\right)^{-\alpha}}{1-\left(1+\frac{\beta}{x}\right)^{-\alpha}}\right)^{\lambda}. \tag{19}$$

Figure 3 displays the HF of the MKILD for selected parameter values. The plots reveal that the MKILD accommodates a variety of failure rate behaviours. Specifically, depending on the choice of the shape parameters α and λ, the HF exhibits strictly increasing shapes (characteristic of wear-out failures), as well as decreasing shapes (typical of early-life or burn-in failures) hazard rates. This flexibility is particularly valuable in reliability engineering and biomedical studies, where different phases of a system's life cycle may exhibit such failure patterns.

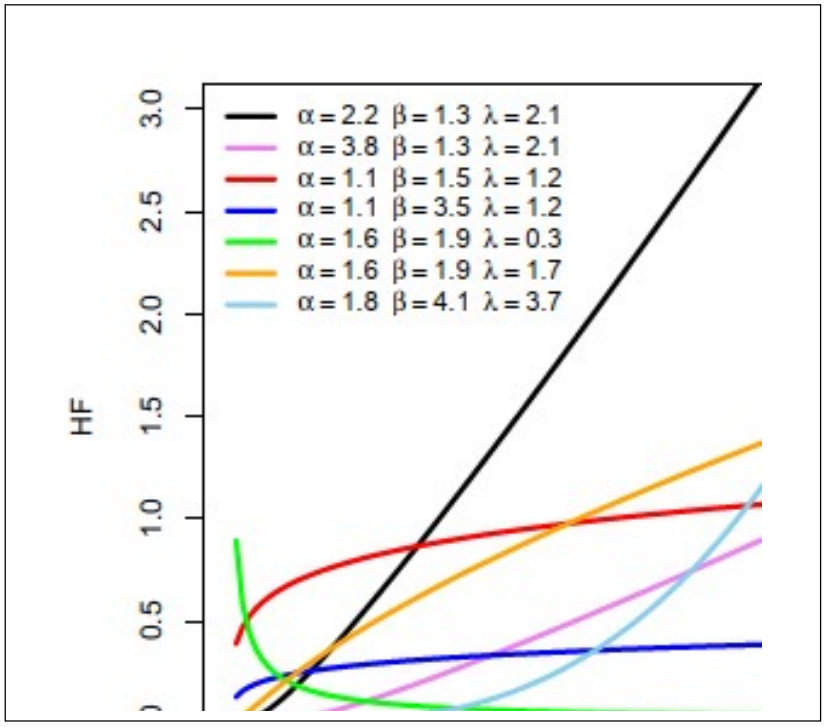


Figure 3: The HF plots of the MKILD.

4. Estimations

The estimation of the unknown parameters of the MKILD are investigated using different approaches. Hereafter, let $x_i = x_1, x_2, \ldots, x_n$ be a random sample of n size and $x_{(i)} = x_{(1)}, x_{(2)}, \ldots, x_{(n)}$ be their values in ascending order; taken from the random variable $X \sim \text{MKILD}(\Phi)$, where $\Phi = (\alpha, \beta, \lambda)$.

4.1 Maximum Likelihood Estimation (MLE)

The log-likelihood function, denoted by ℓ, based on a complete sample for the unknown parameters of the MKILD can be expressed as:

$$\ell(\Phi) = n\,ln\,\alpha + n\,ln\,\beta + n\,ln\,\lambda - 2\sum_{i=1}^{n} ln\,x_i - (\alpha\lambda + 1)\sum_{i=1}^{n} ln\left[1 - \left(1 + \frac{\beta}{x_i}\right)^{-\alpha}\right] - \sum_{i=1}^{n}\left[\frac{\left(1 + \frac{\beta}{x_i}\right)^{-\alpha}}{1 - \left(1 + \frac{\beta}{x_i}\right)^{-\alpha}}\right]^{\lambda}. \tag{20}$$

The partial derivatives of Equation (25) with respect to α, β and λ can be obtained as follows:

$$\frac{\partial \ell}{\partial \alpha} = \frac{n}{\alpha} - \lambda\sum_{i=1}^{n} ln\left[\left(1 + \frac{\beta}{x_i}\right)\right] + (\lambda + 1)\sum_{i=1}^{n}\left[\frac{\left(1 + \frac{\beta}{x_i}\right)^{-\alpha} ln\left(1 + \frac{\beta}{x_i}\right)}{\left(1 - \left(1 + \frac{\beta}{x_i}\right)^{-\alpha}\right)^2}\right] + \lambda\sum_{i=1}^{n}\left[\left(\frac{\left(1 + \frac{\beta}{x_i}\right)^{-\alpha}}{1 - \left(1 + \frac{\beta}{x_i}\right)^{-\alpha}}\right)^{\lambda-1} \frac{\left(1 + \frac{\beta}{x_i}\right)^{-\alpha} ln\left(1 + \frac{\beta}{x_i}\right)}{\left(1 - \left(1 + \frac{\beta}{x_i}\right)^{-\alpha}\right)^2}\right], \tag{21}$$

$$\frac{\partial \ell}{\partial \beta} = \frac{n}{\beta} - (\alpha\lambda + 1)\sum_{i=1}^{n}\left[\frac{1}{x_i + \beta}\right] + (\lambda + 1)\sum_{i=1}^{n}\left[\frac{\alpha\left(1 + \frac{\beta}{x_i}\right)^{-\alpha}}{(x_i + \beta)\left(1 - \left(1 + \frac{\beta}{x_i}\right)^{-\alpha}\right)}\right] + \lambda\sum_{i=1}^{n}\left[\left(\frac{\left(1 + \frac{\beta}{x_i}\right)^{-\alpha}}{1 - \left(1 + \frac{\beta}{x_i}\right)^{-\alpha}}\right)^{\lambda-1} \frac{\alpha\left(1 + \frac{\beta}{x_i}\right)^{-\alpha}}{(x_i + \beta)\left(1 - \left(1 + \frac{\beta}{x_i}\right)^{-\alpha}\right)^2}\right], \tag{22}$$

and

$$\frac{\partial \ell}{\partial \lambda} = \frac{n}{\lambda} - \alpha\sum_{i=1}^{n}\left[ln\left(1 + \frac{\beta}{x_i}\right)\right] - \sum_{i=1}^{n}\left[ln\left(1 - \left(1 + \frac{\beta}{x_i}\right)^{-\alpha}\right)\right] - \sum_{i=1}^{n}\left[\left(\frac{\left(1 + \frac{\beta}{x_i}\right)^{-\alpha}}{1 - \left(1 + \frac{\beta}{x_i}\right)^{-\alpha}}\right)^{\lambda} ln\left(\frac{\left(1 + \frac{\beta}{x_i}\right)^{-\alpha}}{1 - \left(1 + \frac{\beta}{x_i}\right)^{-\alpha}}\right)\right]. \tag{23}$$

For the MLEs $(\hat{\alpha}, \hat{\beta}, \hat{\lambda})$, set the partial derivatives equal to zero: $\frac{\partial \ell}{\partial \alpha}, \frac{\partial \ell}{\partial \beta}, \frac{\partial \ell}{\partial \lambda} = 0$. These equations cannot be solved analytically, so numerical optimisation is required to obtain $\hat{\alpha}, \hat{\beta}, \hat{\lambda}$.

4.2 Least Square Estimation (LSE)

The LS estimates; $\hat{\alpha}_{LSE}$, $\hat{\beta}_{LSE}$, and $\hat{\lambda}_{LSE}$, of $\alpha, \beta,$ and λ respectively, are obtained by minimizing:

$$L = \sum_{i=1}^{n}\left[1 - exp\left[-\left(\frac{\left(1+\frac{\beta}{x_{(i)}}\right)^{-\alpha}}{1-\left(1+\frac{\beta}{x_{(i)}}\right)^{-\alpha}}\right)^{\lambda}\right] - \frac{i}{n+1}\right]^{2}. \tag{24}$$

4.3 Weighted Least Square Estimation (WLSE)

The WLS estimates; $\hat{\alpha}_{WLSE}$, $\hat{\beta}_{WLSE}$, and $\hat{\lambda}_{WLSE}$, of α, β and λ respectively, are obtained by minimizing:

$$W = \sum_{i=1}^{n}\frac{(n+1)^2(n+2)}{i(n-i+1)}\sum_{i=1}^{n}\left[1 - exp\left[-\left(\frac{\left(1+\frac{\beta}{x_{(i)}}\right)^{-\alpha}}{1-\left(1+\frac{\beta}{x_{(i)}}\right)^{-\alpha}}\right)^{\lambda}\right] - \frac{i}{n+1}\right]^{2}. \tag{25}$$

4.4 Maximum Product of Spacings Estimation (MPSE)

The MPS estimates; $\hat{\alpha}_{MPSE}$, $\hat{\beta}_{MPSE}$, and $\hat{\lambda}_{MPSE}$, of $\alpha, \beta,$ and λ are respectively obtained by maximizing:

$$M = \frac{1}{n+1} + \sum_{i=1}^{n+1} log\left[\left\{1 - exp\left[-\left(\frac{\left(1+\frac{\beta}{x_{(i)}}\right)^{-\alpha}}{1-\left(1+\frac{\beta}{x_{(i)}}\right)^{-\alpha}}\right)^{\lambda}\right]\right\} - \left\{1 - exp\left[-\left(\frac{\left(1+\frac{\beta}{x_{(i-1)}}\right)^{-\alpha}}{1-\left(1+\frac{\beta}{x_{(i-1)}}\right)^{-\alpha}}\right)^{\lambda}\right]\right\}\right]^{2}. \tag{26}$$

4.5 Anderson-Darling Estimation (ADE)

The AD estimates; $\hat{\alpha}_{ADE}$, $\hat{\beta}_{ADE}$, and $\hat{\lambda}_{ADE}$, of $\alpha, \beta,$ and λ are respectively obtained by minimizing:

$$A = -n - \frac{1}{n}\sum_{i=1}^{n}\left[(2i-1)\ln\left(1 - exp\left[-\left(\frac{\left(1+\frac{\beta}{x_{(i)}}\right)^{-\alpha}}{1-\left(1+\frac{\beta}{x_{(i)}}\right)^{-\alpha}}\right)^{\lambda}\right]\right) - (2n+1-2i)\left(\frac{\left(1+\frac{\beta}{x_{(i)}}\right)^{-\alpha}}{1-\left(1+\frac{\beta}{x_{(i)}}\right)^{-\alpha}}\right)^{\lambda}\right]. \tag{27}$$

4.6 Cramér-von Mises Estimation (CVME)

The CVM estimates; $\hat{\alpha}_{CVME}$, $\hat{\beta}_{CVME}$, and $\hat{\lambda}_{CVME}$, of $\alpha, \beta,$ and λ respectively, are obtained by minimizing:

$$C = \sum_{i=1}^{n}\left[1 - exp\left[-\left(\frac{\left(1+\frac{\beta}{x_{(i)}}\right)^{-\alpha}}{1-\left(1+\frac{\beta}{x_{(i)}}\right)^{-\alpha}}\right)^{\lambda}\right] - \frac{2i-1}{2n}\right]^{2} + \frac{1}{12n}. \quad (28)$$

Equations (21) - (28) involve non-linear functions, hence, require numerical optimization techniques to minimize or maximize the respective objective functions. In this study, the *R* statistical software was employed.

5. Numerical illustration

This section investigates the finite-sample performance and asymptotic behaviour of the estimators of the parameters of the MKILD through an extensive Monte Carlo simulation study. The simulation experiment was repeated 1000 times for different sample sizes $n = 25, 50, 100, 150, 200,$ and 250. Three different parameter configurations were considered in order to assess the robustness and stability of the competing estimation procedures under varying distributional shapes. The simulation algorithm follows these steps:

1. Specify the number of Monte Carlo replications, $N = 1000$;
2. Select the true parameter values of the MKILD;
3. Generate a random sample of size n from the MKILD;
4. Estimate the unknown parameters using the ADE, CVME, LSE, MLE, MPSE,and WLSE methods;
5. Repeat Steps (3) - (4) independently N times;
6. Compute the average bias and mean squared error (MSE) for each estimator.

For each simulated sample, parameter estimation was carried out using the L-BFGS-B optimisation algorithm implemented in R software. Positive lower bounds were imposed on the parameter space to guarantee admissible estimates and numerical stability throughout the optimisation process.

The simulation results for the different parameter settings are reported in Tables 2 - 4. A careful examination of the numerical results leads to the following observations:

1. Consistency of the estimators. All six estimation methods exhibit consistency since the biases and MSEs generally decrease as n increases across all parameter settings.
2. Superiority of the MLE. The MLE provides the most stable and efficient overall performance by consistently producing the smallest or near-smallest biases and MSEs, particularly for moderate and large n.
3. Performance of the MPSE. The MPSE performs competitively with highly accurate estimates for large n, although it exhibits relatively large MSEs for some parameters in small n.
4. Performance of the ADE and WLSE. The ADE and WLSE show moderate but stable performances with steadily improving biases and MSEs as n increases.
5. Behaviour of the CVME and LSE. The CVME and LSE generally produce comparatively larger biases and MSEs, especially for small n, despite improving with increasing n.
6. Effect of sample size. The estimation accuracy of all methods improves substantially with increasing n, confirming their asymptotic reliability for the MKILD.

For researchers working with the MKILD, the MLE is strongly recommended as the default estimation technique while the MPSE also provides competitive performance, hence, can be considered particularly for moderate and large samples.

Table 2: The Biases and MSEs (in parenthesis) of the MKILD at $(\alpha = 0.9, \beta = 0.1, \lambda = 1.2)$.

Method↓	***n*→**	**25**	**50**	**100**	**150**	**200**	**250**
	$\hat{\alpha}$	0.770(4.012)	0.274(1.250)	0.117(0.351)	0.064(0.177)	0.066(0.127)	0.025(0.087)
ADE	$\hat{\beta}$	0.327(0.483)	0.254(0.373)	0.126(0.178)	0.085(0.120)	0.037(0.046)	0.027(0.014)
	$\hat{\lambda}$	0.396(0.785)	0.295(0.516)	0.146(0.234)	0.101(0.149)	0.051(0.074)	0.051(0.048)
	$\hat{\alpha}$	0.292(1.060)	0.137(0.640)	0.066(0.326)	0.057(0.256)	0.050(0.178)	0.010(0.140)
CVME	$\hat{\beta}$	0.254(0.238)	0.221(0.183)	0.136(0.100)	0.109(0.074)	0.074(0.045)	0.075(0.040)
	$\hat{\lambda}$	0.393(0.662)	0.316(0.447)	0.206(0.266)	0.165(0.207)	0.119(0.142)	0.133(0.132)
	$\hat{\alpha}$	0.060(0.682)	-0.001(0.498)	-0.005(0.283)	0.004(0.227)	0.017(0.163)	-0.030(0.134)
LSE	$\hat{\beta}$	0.298(0.247)	0.257(0.194)	0.154(0.100)	0.116(0.068)	0.079(0.042)	0.076(0.035)
	$\hat{\lambda}$	0.471(0.646)	0.387(0.477)	0.246(0.280)	0.190(0.210)	0.135(0.143)	0.142(0.129)
	$\hat{\alpha}$	0.481(2.846)	0.115(0.742)	0.087(0.305)	0.012(0.115)	0.002(0.077)	0.006(0.069)
MLE	$\hat{\beta}$	0.426(0.682)	0.285(0.465)	0.168(0.410)	0.087(0.116)	0.056(0.079)	0.037(0.024)
	$\hat{\lambda}$	0.443(0.818)	0.302(0.486)	0.142(0.244)	0.095(0.126)	0.066(0.076)	0.056(0.055)
	$\hat{\alpha}$	0.284(1.772)	0.143(0.604)	0.133(0.267)	0.089(0.122)	0.088(0.108)	0.071(0.072)
MPSE	$\hat{\beta}$	0.406(0.659)	0.278(0.752)	0.140(0.493)	0.044(0.096)	0.036(0.095)	0.016(0.017)
	$\hat{\lambda}$	0.359(0.657)	0.214(0.397)	0.075(0.201)	0.015(0.074)	0.006(0.063)	0.001(0.035)
	$\hat{\alpha}$	0.829(2.120)	0.449(0.991)	0.263(0.457)	0.202(0.348)	0.180(0.316)	0.124(0.297)
WLSE	$\hat{\beta}$	0.045(0.072)	0.030(0.037)	0.012(0.011)	0.008(0.005)	0.007(0.005)	0.017(0.005)
	$\hat{\lambda}$	0.034(0.163)	0.034(0.108)	0.017(0.062)	0.010(0.042)	0.011(0.038)	0.035(0.041)

Table 3: The Biases and MSEs (in parenthesis) of the MKILD at $(\alpha = 1.1, \beta = 0.2, \lambda = 0.6)$.

Method↓	***n*→**	**25**	**50**	**100**	**150**	**200**	**250**
	$\hat{\alpha}$	0.658(7.325)	0.113(0.576)	0.055(0.140)	0.034(0.084)	0.039(0.068)	0.015(0.048)
ADE	$\hat{\beta}$	1.284(53.431)	0.571(18.566)	0.090(1.565)	0.021(0.010)	0.024(0.159)	0.013(0.005)
	$\hat{\lambda}$	0.192(0.245)	0.096(0.095)	0.024(0.017)	0.012(0.005)	0.008(0.005)	0.009(0.003)
	$\hat{\alpha}$	0.689(4.418)	0.255(1.205)	0.100(0.283)	0.051(0.199)	0.060(0.143)	0.032(0.097)
CVME	$\hat{\beta}$	0.565(2.015)	0.308(0.834)	0.100(0.193)	0.061(0.058)	0.033(0.030)	0.028(0.019)
	$\hat{\lambda}$	0.168(0.186)	0.100(0.088)	0.037(0.027)	0.027(0.015)	0.017(0.010)	0.014(0.007)
	$\hat{\alpha}$	0.264(2.586)	0.073(0.877)	0.019(0.242)	0.000(0.183)	0.022(0.132)	0.002(0.092)
LSE	$\hat{\beta}$	0.798(2.588)	0.420(1.131)	0.136(0.263)	0.081(0.083)	0.044(0.035)	0.036(0.023)
	$\hat{\lambda}$	0.256(0.241)	0.146(0.111)	0.056(0.033)	0.040(0.018)	0.025(0.011)	0.020(0.008)
	$\hat{\alpha}$	0.509(6.334)	0.072(0.380)	0.030(0.160)	0.012(0.074)	0.002(0.053)	0.007(0.042)
MLE	$\hat{\beta}$	0.926(6.274)	0.501(4.761)	0.122(0.179)	0.055(0.015)	0.047(0.011)	0.037(0.007)
	$\hat{\lambda}$	0.226(0.233)	0.128(0.097)	0.057(0.020)	0.034(0.006)	0.031(0.005)	0.024(0.004)
	$\hat{\alpha}$	0.203(1.307)	0.162(0.842)	0.118(0.174)	0.097(0.092)	0.060(0.063)	0.069(0.054)
MPS	$\hat{\beta}$	1.910(125.612)	0.725(27.584)	0.077(0.134)	0.028(0.009)	0.028(0.008)	0.019(0.005)
	$\hat{\lambda}$	0.207(0.248)	0.092(0.100)	0.025(0.013)	0.010(0.004)	0.014(0.004)	0.007(0.003)
	$\hat{\alpha}$	0.567(3.315)	0.178(0.716)	0.071(0.168)	0.036(0.116)	0.044(0.085)	0.022(0.060)
WLSE	$\hat{\beta}$	0.463(1.774)	0.212(0.620)	0.050(0.066)	0.032(0.021)	0.015(0.010)	0.015(0.007)
	$\hat{\lambda}$	0.156(0.167)	0.086(0.066)	0.028(0.015)	0.020(0.008)	0.013(0.005)	0.011(0.004)

Table 4: The Biases and MSEs (in parenthesis) of the MKILD at ($\alpha = 1, \beta = 0.3, \lambda = 0.9$).

Method↓	***n*→**	**25**	**50**	**100**	**150**	**200**	**250**
	$\hat{\alpha}$	1.413(18.818)	0.269(1.374)	0.089(0.266)	0.059(0.148)	0.052(0.103)	0.036(0.067)
ADE	$\hat{\beta}$	1.234(13.575)	0.655(6.147)	0.231(1.433)	0.106(0.496)	0.061(0.281)	0.025(0.020)
	$\hat{\lambda}$	0.287(0.494)	0.157(0.237)	0.071(0.076)	0.041(0.037)	0.024(0.023)	0.016(0.011)
	$\hat{\alpha}$	0.999(6.520)	0.457(2.011)	0.195(0.715)	0.123(0.351)	0.098(0.238)	0.063(0.158)
CVME	$\hat{\beta}$	0.830(3.155)	0.521(1.675)	0.299(0.790)	0.183(0.443)	0.129(0.273)	0.085(0.126)
	$\hat{\lambda}$	0.257(0.391)	0.165(0.224)	0.105(0.115)	0.066(0.069)	0.048(0.051)	0.038(0.033)
	$\hat{\alpha}$	0.435(3.567)	0.207(1.354)	0.083(0.566)	0.053(0.301)	0.048(0.212)	0.024(0.145)
LSE	$\hat{\beta}$	1.118(3.785)	0.694(2.042)	0.386(0.938)	0.227(0.496)	0.158(0.296)	0.111(0.153)
	$\hat{\lambda}$	0.380(0.470)	0.240(0.269)	0.147(0.137)	0.091(0.079)	0.067(0.057)	0.053(0.038)
	$\hat{\alpha}$	0.746(8.059)	0.178(1.575)	0.060(0.236)	0.024(0.103)	0.002(0.077)	0.003(0.059)
MLE	$\hat{\beta}$	1.558(14.722)	0.956(8.655)	0.331(3.324)	0.116(0.358)	0.117(0.560)	0.097(0.728)
	$\hat{\lambda}$	0.338(0.515)	0.207(0.280)	0.086(0.097)	0.043(0.031)	0.041(0.029)	0.034(0.022)
	$\hat{\alpha}$	0.478(5.841)	0.188(0.946)	0.142(0.246)	0.114(0.126)	0.073(0.084)	0.073(0.071)
MPS	$\hat{\beta}$	2.179(69.585)	0.973(15.972)	0.288(7.070)	0.033(0.032)	0.036(0.030)	0.024(0.021)
	$\hat{\lambda}$	0.275(0.456)	0.135(0.229)	0.031(0.077)	0.004(0.015)	0.002(0.014)	0.003(0.010)
	$\hat{\alpha}$	0.846(5.237)	0.343(1.415)	0.128(0.357)	0.088(0.194)	0.067(0.131)	0.043(0.082)
WLSE	$\hat{\beta}$	0.683(2.695)	0.346(1.175)	0.166(0.425)	0.094(0.208)	0.054(0.085)	0.033(0.031)
	$\hat{\lambda}$	0.235(0.353)	0.130(0.167)	0.073(0.069)	0.046(0.039)	0.030(0.025)	0.023(0.015)

6. Real Data Applications

This Section provides real applications to three real-life datasets to illustrate the flexibility of the MKILD compared to the Inverse Lomax distribution and some of its generalisations (for all $x > 0, \alpha > 0, \beta > 0$ and $\lambda > 0$) namely

- Inverse Lomax (IL)

$$f(x) = \alpha\beta x^{-2}\left(1 + \frac{\beta}{x}\right)^{-(\alpha+1)}.$$

- Power IL (PIL) by Hassan *et al.* (2021)

$$f(x) = \lambda\alpha\beta x^{\alpha\lambda-1}(\beta + x^{\lambda})^{-(\alpha+1)}.$$

- Marshall-Olkin IL (MOIL) by Maxwell *et al.* (2019)

$$f(x) = \frac{\lambda\alpha\beta x^{-2}\left(1 + \frac{\beta}{x}\right)^{-(\alpha+1)}}{\left[1 - (1-\lambda)\left(1 - \left(1 + \frac{\beta}{x}\right)^{-\alpha}\right)\right]^{2}}.$$

- Exponentiated Generalized IL (EGIL) by Bashiru and Itopa (2023)

$$f(x) = \lambda\theta\left[1 - \left(1 + \frac{\beta}{x}\right)^{-\alpha}\right]^{\lambda-1}\left[1 - \left(1 - \left(1 + \frac{\beta}{x}\right)^{-\alpha}\right)^{\lambda}\right]^{\theta-1}\alpha\beta x^{-2}\left(1 + \frac{\beta}{x}\right)^{-(\alpha+1)}.$$

- Odd Fréchet IL (OFIL) by ZeinEldin *et al.* (2020)

$$f(x) = \left(\left(1 + \frac{\beta}{x}\right)^{-\alpha}\right)^{-\lambda-1}\lambda\left(\alpha\beta x^{-2}\left(1 + \frac{\beta}{x}\right)^{-\alpha-1}\right)\left[1 - \left(1 + \frac{\beta}{x}\right)^{-\alpha}\right]^{\lambda-1} exp\left[-\left(\frac{1 - \left(1 + \frac{\beta}{x}\right)^{-\alpha}}{\left(1 + \frac{\beta}{x}\right)^{-\alpha}}\right)^{\lambda}\right].$$

The first dataset comprises the breaking stress (in GPa) of carbon fibres with a gauge length of 50 mm, as originally reported by Nicholas and Padgett (2006). This dataset was subsequently analyzed by Bashiru and Itopa (2023). The second dataset pertains to COVID-19 mortality rates in Mexico, consisting of 106 daily observations collected between March 4, 2020, and July 20, 2020, as utilized by Ehizojie (2026). The third dataset contains measurements of the tensile strength (in GPa) of 69 carbon fibres tested under tension at a gauge length of 20 mm, as documented by Ghitany *et al.* (2013). The datasets are presented below:

Dataset 1	0.39,	0.85,	1.08,	1.25,	1.47,	1.57,	1.61,	1.61,	1.69,	1.80,
	1.84,	1.87,	1.89,	2.03,	2.03,	2.05,	2.12,	2.35,	2.41,	2.43,
	2.48,	2.50,	2.53,	2.55,	2.55,	2.56,	2.59,	2.67,	2.73,	2.74,
	2.79,	2.81,	2.82,	2.85,	2.87,	2.88,	2.93,	2.95,	2.96,	2.97,
	3.09,	3.11,	3.11,	3.15,	3.15,	3.19,	3.22,	3.22,	3.27,	3.28,
	3.31,	3.31,	3.33,	3.39,	3.39,	3.56,	3.60,	3.65,	3.68,	3.70,
	3.75,	4.20,	4.38,	4.42,	4.70,	4.90.				
Dataset 2	8.826,	6.105,	9.391,	14.962,	10.383,	7.267,	13.220,	16.498,	11.665,	6.015,
	10.855,	6.122,	6.656,	3.440,	5.854,	10.685,	10.035,	5.242	4.344,	5.143,
	7.630,	14.604,	7.903,	6.370,	3.537,	6.327,	4.730,	3.215,	9.284,	12.878,
	8.813,	10.043,	7.260,	5.985,	6.412,	3.395,	4.424,	9.935,	7.840,	9.550,
	3.499,	3.751,	6.968,	3.286,	10.158,	8.108,	6.697,	7.151,	6.560,	2.077,
	3.778,	2.988,	3.336,	6.814,	8.325,	7.854,	8.551,	3.228,	7.486,	6.625,
	6.140,	4.909,	4.661,	5.392,	12.042,	8.696,	1.815,	3.327,	5.406,	6.182,
	1.041	1.800,	4.949,	4.089,	3.359,	2.070,	3.298,	5.317,	5.442	4.557,
	4.292,	2.500,	6.535,	4.648,	4.697,	5.459,	4.120,	3.922,	3.219,	1.402,
	2.438,	3.257,	3.632,	3.233,	3.027,	2.352,	1.205,	3.218,	2.926,	2.601,
	2.065,	3.029,	2.058,	2.326,	2.506,	1.923.				
Dataset 3	1.312,	1.314,	1.479,	1.552,	1.700,	1.803,	1.861,	1.865,	1.944,	1.958,
	1.966,	1.997,	2.006,	2.021	2.027,	2.055,	2.063,	2.098,	2.140,	2.179,
	2.224,	2.240,	2.253,	2.270,	2.272,	2.274,	2.301,	2.301,	2.359,	2.382,
	2.382,	2.426,	2.434,	2.435,	2.478,	2.490,	2.511,	2.514,	2.535,	2.554,
	2.566,	2.570,	2.586,	2.629,	2.633,	2.642,	2.648,	2.684,	2.697,	2.726,
	2.770,	2.773,	2.800,	2.809,	2.818,	2.821,	2.848,	2.880,	2.954,	3.012,
	3.067,	3.084,	3.090,	3.096,	3.128,	3.233,	3.433,	3.585,	3.585.	

The descriptive statistics and box plots for the data are given in Table 2 and Figure 4 respectively. It can be seen that first and third data exhibit negative skewness, while the second data is positively skewed with first and second data containing outliers suggesting a leptokurtic distribution. The MKILD effectively captures these distributional features, as illustrated by the PDF plots in Figure 1. Therefore, the MKILD can be good a choice to model these datasets.

The ML method is performed to obtain the point estimates and their standard errors (SEs) of the model parameters. To compare and select the best model, some discrimination criteria are applied which include; log-likelihood function (ℓ) evaluated at the parameter estimates, Akaike information criterion (AIC), Bayesian information criterion (BIC), consistent Akaike information criterion (CAIC), and Hannan-Quinn information criterion (HQIC). In addition to the discrimination criteria, various goodness-of-fit test statistics such as Cramér-von Mises (W*), Anderson-Darling (A*), and Kolmogorov-Smirnov (KS) statistics, along with the corresponding KS *p*-value are employed to determine the model with the best fit for the data. The best model is the one that has the lowest values of, AIC, CAIC, BIC, HQIC, W*, A*, and KS; the highest KS *p*-value.

The results for these measures to the considered models are reported in Table 6, 7 and 8. The analyses reveal that the MKILD produce favourable fit relative to other competing models considered in this study when applied to the provided datasets; this superiority is further corroborated by fitted densities, fitted CDFs, probability-probability (PP) plots, and quantile-quantile (QQ) plots as displayed in Figures 5, 6, and 7. Thus, the MKILD provides a more flexible alternative to existing models for analysing lifetime data.

To identify the best estimators for the datasets, several estimation techniques have been applied for this purpose. Table 9 reports the various estimators for datasets based on different estimation approaches. It is noted that all methods work quite well for analysing the data, however, the LSE, WLSE and LSE are the best techniques for the first, second and third datasets respectively.

Table 5: Descriptive statistics of the datasets.

Dataset	***n***	**Mean**	**Median**	**Mode**	**Min**	**Max**	**SD**	**Skewness**	**Kurtosis**
Dataset 1	66	2.7595	2.8350	1.6100	0.3900	4.9000	0.8915	-0.1315	3.2230
Dataset 2	106	5.8223	5.2795	8.8260	1.0410	16.4980	3.2499	0.9732	3.6661
Dataset 3	69	2.4513	2.4780	2.3010	1.3120	3.5850	0.4951	-0.0282	2.9407

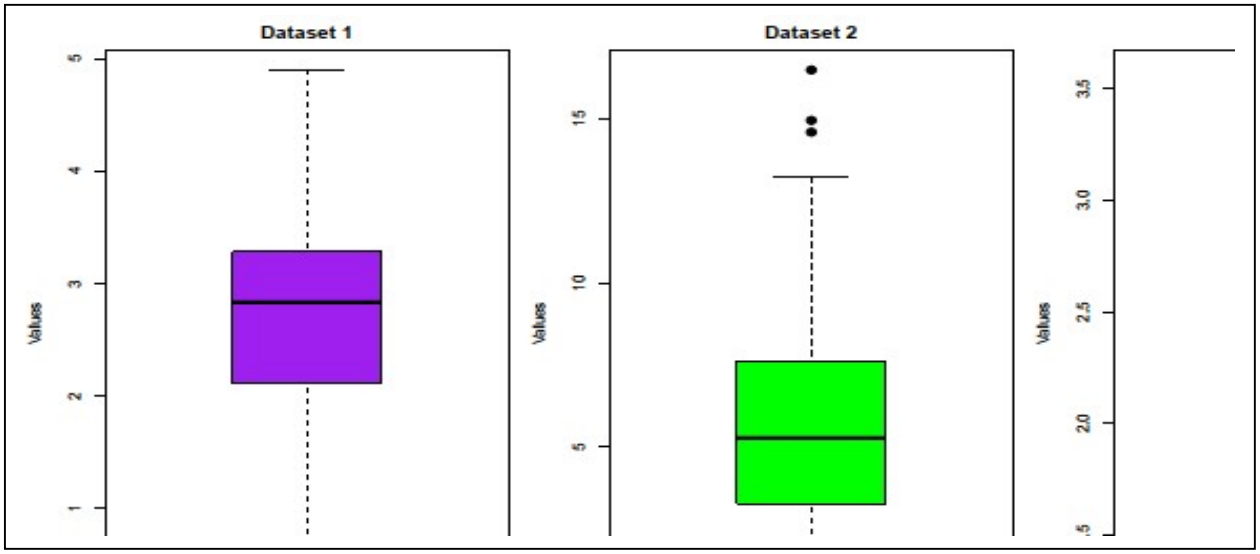


Figure 4: The box plots for the three datasets.

Table 6: The MLEs, SEs, discrimination criteria and goodness-of-fit statistics for Dataset 1.

Statistic↓ Model→	**MKIL**	**OFIL**	**EGIL**	**MOIL**	**PIL**	**IL**
$\hat{\alpha}$	0.8364	0.4218	5.2205	6.5326	1.2760	16.2372
$\hat{\beta}$	3.9594	8.5069	2.6647	4.1528	25.2117	0.1436
$\hat{\lambda}$	3.6971	2.6241	31.3110	0.0021	3.7242	-
$\hat{\theta}$	-	-	1.1919	-	-	-
SE($\hat{\alpha}$)	0.6012	0.0770	1.6663	0.8323	0.2612	8.0790
SE($\hat{\beta}$)	4.2135	3.1773	1.0466	0.8332	11.6626	0.0743
SE($\hat{\lambda}$)	1.0763	0.3691	14.0828	0.0003	0.3391	-
SE($\hat{\theta}$)	-	-	0.3808	-	-	-
$\hat{\ell}$	**85.9542**	115.1974	90.8771	97.6167	95.2420	137.1333
AIC	**177.9083**	236.3949	189.7541	201.2334	196.4840	278.2666
BIC	**184.4773**	242.9638	198.5127	207.8024	203.0530	282.6459
CAIC	**178.2954**	236.7819	190.4099	201.6205	196.8711	278.4571
HQIC	**180.5040**	238.9906	193.2151	203.8291	199.0797	279.9970
W*	**0.0882**	0.8062	0.2305	0.4160	0.3550	0.6251
A*	**0.5066**	4.5481	1.2430	2.2718	1.9253	3.5228
KS	**0.0784**	0.2049	0.1413	0.1407	0.1531	0.3809
KS (p-value)	**0.8115**	0.0078	0.1432	0.1464	0.0908	0.0000

Table 7: The MLEs, SEs, discrimination criteria and goodness-of-fit statistics for Dataset 2.

Statistic↓ Model→	**MKIL**	**OFIL**	**EGIL**	**MOIL**	**PIL**	**IL**
$\hat{\alpha}$	7.2929	0.5482	4.4599	5.3783	2.5546	10.5061
$\hat{\beta}$	0.6254	9.3608	3.4602	5.6096	8.8346	0.4116
$\hat{\lambda}$	1.3703	2.1667	7.3696	0.0164	2.1632	-
$\hat{\theta}$	-	-	1.1476	-	-	-
SE($\hat{\alpha}$)	2.3724	0.0837	-	1.3561	0.5826	4.0976
SE($\hat{\beta}$)	0.2157	2.5510	2.4566	3.1359	3.4630	0.1705
SE($\hat{\lambda}$)	0.1029	0.2268	6.4765	0.0117	0.1557	-
SE($\hat{\theta}$)	-	-	1.1413	-	-	-
$\hat{\ell}$	**261.2652**	270.5633	262.4447	269.2723	267.3846	297.4709
AIC	**528.5304**	547.1266	532.8895	544.5445	540.7693	598.9418
BIC	**536.5207**	555.1170	543.5432	552.5348	548.7596	604.2687
CAIC	**528.7657**	547.3619	533.2855	544.7798	541.0046	599.0583
HQIC	**531.7689**	550.3652	537.2075	547.7830	544.0078	601.1008
W*	**0.0442**	0.2122	0.0657	0.2063	0.1607	0.1381
A*	**0.2534**	1.3539	0.3651	1.2338	0.9732	0.8591
KS	**0.0538**	0.0955	0.0766	0.0856	0.0927	0.2576
KS (p-value)	**0.9193**	0.2886	0.5621	0.4191	0.3223	0.0000

Table 8: The MLEs, SEs, discrimination criteria and goodness-of-fit statistics for Dataset 3.

Statistic↓ Model→	**MKIL**	**OFIL**	**EGIL**	**MOIL**	**PIL**	**IL**
$\hat{\alpha}$	3.7910	0.7206	9.9438	7.6997	3.2069	10.1732
$\hat{\beta}$	0.5294	3.4460	0.4597	2.8800	21.1011	0.2265
$\hat{\lambda}$	4.4351	4.7287	12.2321	0.0022	5.1413	-
$\hat{\theta}$	-	-	6.8098	-	-	-
SE($\hat{\alpha}$)	0.9707	0.1295	2.5599	0.6575	1.1528	3.4808
SE($\hat{\beta}$)	0.1486	0.9671	0.1312	0.3546	14.0378	0.0812
SE($\hat{\lambda}$)	0.4106	0.5314	3.1545	0.0003	0.4689	-
SE($\hat{\theta}$)	-	-	2.4101	-	-	-
$\hat{\ell}$	**49.2221**	62.9433	56.1502	70.3180	57.1773	134.1515
AIC	**104.4441**	131.8867	120.3003	146.6359	120.3547	272.3030
BIC	**111.1464**	138.5890	129.2367	153.3382	127.0570	276.7712
CAIC	**104.8134**	132.2559	120.9253	147.0051	120.7239	272.4848
HQIC	**107.1032**	134.5457	123.8457	149.2949	123.0137	274.0756
W*	**0.0259**	0.3572	0.1378	0.1202	0.1922	0.1147
A*	**0.2175**	2.3281	0.9432	0.8151	1.2743	0.7967
KS	**0.0457**	0.1437	0.1118	0.1900	0.1124	0.4638
KS (p-value)	**0.9987**	0.1156	0.3542	0.0138	0.3478	0.0000

Table 9: The AD, CVM, LS, ML, MPS, and WLS estimates for the three datasets.

Dataset	**Method**	$\widehat{\boldsymbol{\alpha}}$	$\widehat{\boldsymbol{\beta}}$	$\hat{\boldsymbol{\lambda}}$	**KS (stat)**	**KS (p-value)**
1	ADE	0.7957	4.2740	3.8917	0.0750	0.8518
	CVME	0.5471	7.8337	5.1240	0.0589	0.9762
	LSE	0.4291	12.3253	5.8129	**0.0533**	**0.9919**
	MLE	0.8364	3.9594	3.6971	0.0784	0.8115
	MPSE	0.6457	5.9142	3.6798	0.1035	0.4797
	WLSE	0.9196	3.4286	3.5373	0.0872	0.6972
2	ADE	11.2280	0.4018	1.3212	0.0535	0.9218
	CVME	2.6528	1.8928	1.5030	0.0536	0.9210
	LSE	3.5465	1.3526	1.4528	0.0505	0.9501
	MLE	7.2929	0.6254	1.3703	0.0538	0.9193
	MPSE	6.3278	0.7414	1.3662	0.0606	0.8310
	WLSE	7.8804	0.5718	1.3483	**0.0501**	**0.9529**
3	ADE	2.8557	0.7228	4.5210	0.0464	0.9984
	CVME	7.5434	0.2531	4.5316	0.0484	0.9969
	LSE	5.1844	0.3746	4.3701	**0.0433**	**0.9995**
	MLE	3.7910	0.5294	4.4351	0.0457	0.9987
	MPSE	3.9529	0.5039	4.1586	0.0588	0.9709
	WLSE	3.2517	0.6221	4.3811	0.0544	0.9867

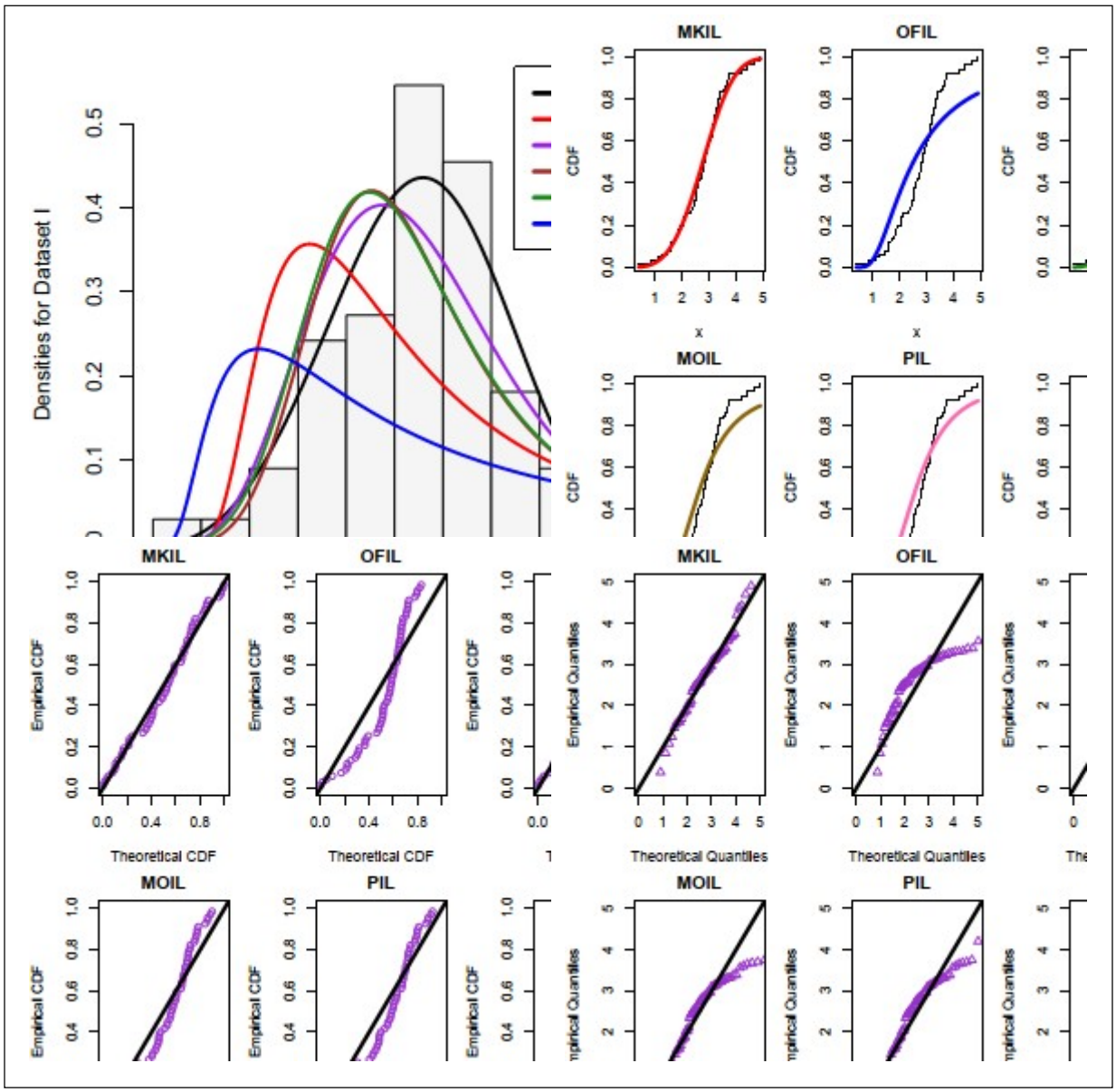


Figure 5: The estimated PDFs (top-left panel), estimated CDFs (top-right panel), PP (bottom-left panel) and QQ (bottom-right panel) plots for Dataset 1.

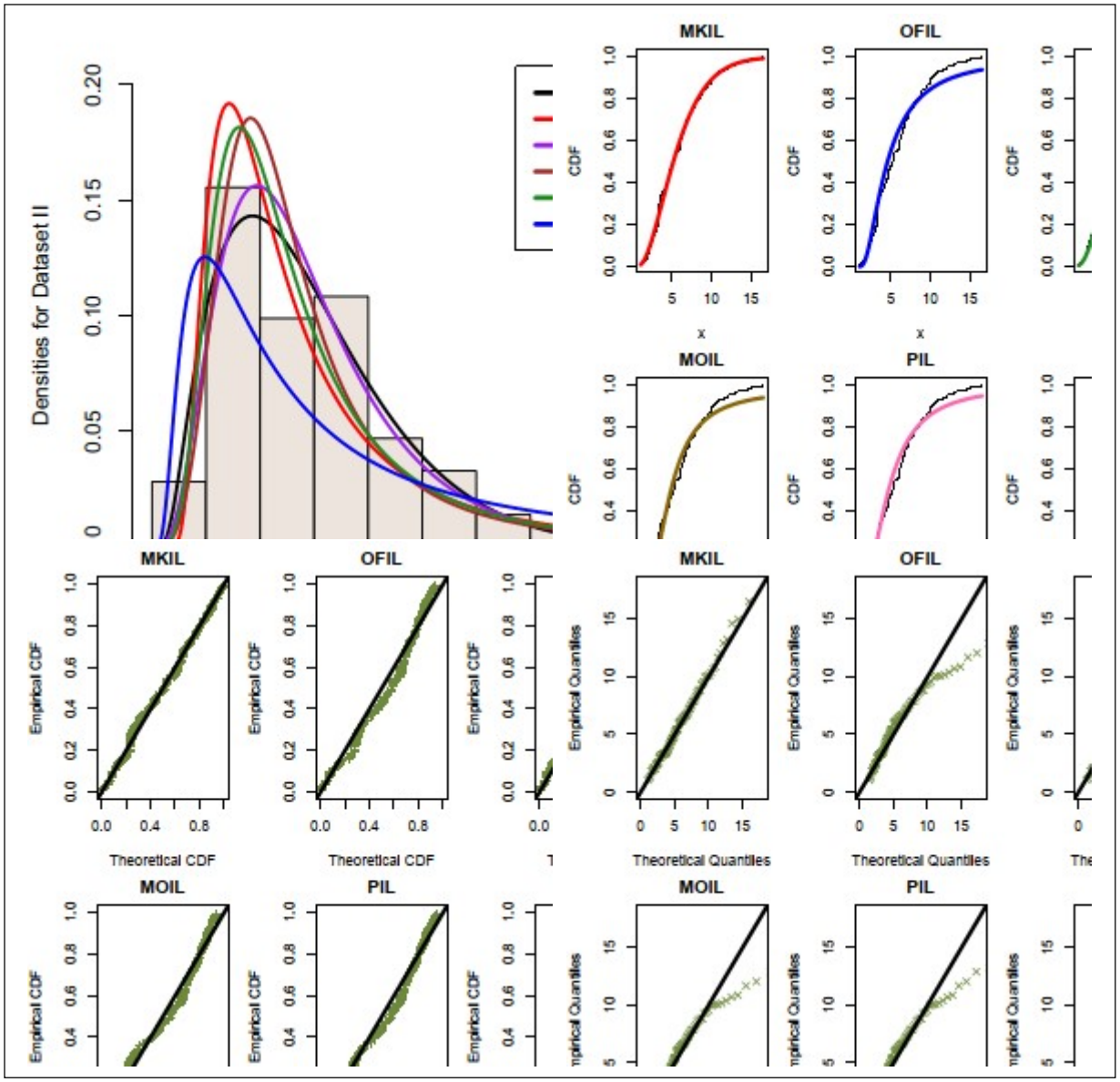


Figure 6: The estimated PDFs (top-left panel), estimated CDFs (top-right panel), PP (bottom-left panel) and QQ (bottom-right panel) plots for Dataset 2.

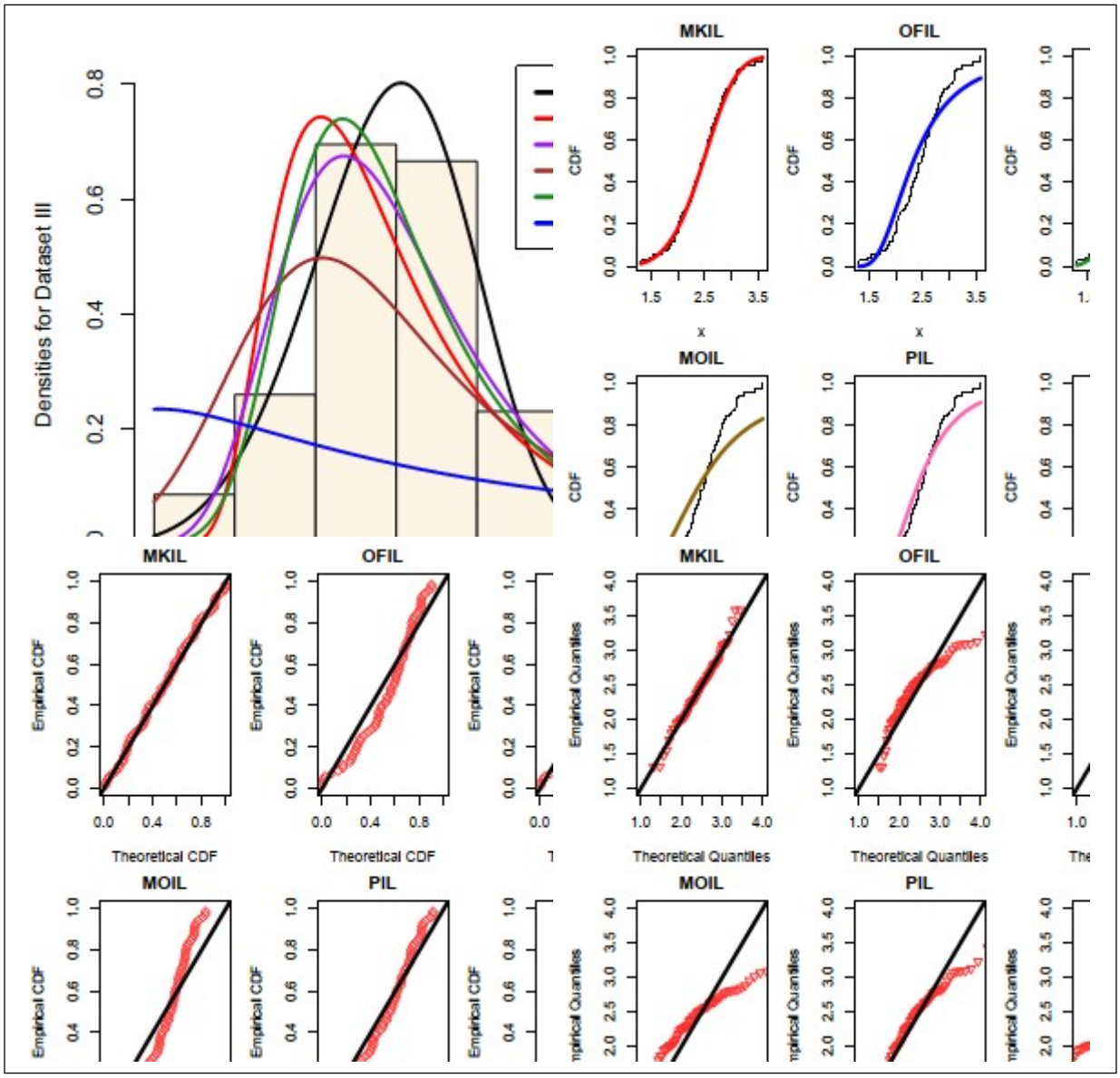


Figure 7: The estimated PDFs (top-left panel), estimated CDFs (top-right panel), PP (bottom-left panel) and QQ (bottom-right panel) plots for Dataset 3.

7. Conclusion

This study has introduced the Modified Kies Inverse Lomax distribution (MKILD) as an extension of the Inverse Lomax distribution (ILD), offering substantially greater flexibility for analysing heavy-tailed lifetime data. The proposed model is distinguished by its adaptable density function, which readily assumes decreasing, nearly symmetric, left- or right-skewed unimodal forms, while its hazard function captures both increasing and decreasing patterns with equal ease. A thorough investigation of key statistical properties, including order statistics, the quantile function, moments, and measures of skewness and kurtosis, establishes a sound theoretical basis for the distribution. Extensive simulation work confirms that all six estimation methods improve consistently with larger samples, with maximum likelihood proving the most efficient and reliable across most scenarios. The practical value of the MKILD is demonstrated through three real-life applications involving heavy-tailed lifetime datasets. In each case, the new model yields favourable fits relative to the ILD and several of its established generalisations, namely the Power ILD, Marshall-Olkin ILD, Exponentiated Generalised ILD, and Odd Fréchet ILD. These empirical results affirm the MKILD's capacity to describe complex lifetime phenomena with precision. Altogether, the MKILD constitutes a robust and versatile addition to the family of heavy-tailed lifetime models, offering statisticians and practitioners a dependable tool for accurate modelling in reliability engineering, survival analysis, and related fields, while opening promising avenues for further extensions and applications.

References

[1]. Adepoju, A. A., Abdulkadir, S. S., Jibasen, D., and Olumoh, J. S. (2024). A Type I half logistic Topp–Leone inverse Lomax distribution with applications in skinfolds analysis. *Reliability: Theory and Applications,* 19(1), 618–630.

[2]. Afere, B. A. E., Daikwo, D. A., Aguda, E. V., Usman, Y. B., Bashiru, S. O., and Bolaji, B. (2026). Modelling maternal blood loss using the exponentiated Kumaraswamy–inverse Lomax distribution. *European Journal of Statistics,* 6, 7–7.

[3]. Al-Babtain, A., Shakhatreh, M. K., Nassar, M., and Afify, A. Z. (2020). A new modified Kies family: Properties, estimation under complete and type-II censored samples, and engineering applications. *Mathematics,* 8(8), 1345. https://doi.org/10.3390/math8081345

[4]. Almarashi, A. M. (2021). A new modified inverse Lomax distribution: Properties, estimation and applications to engineering and medical data. *Computer* Modelling *in Engineering and Sciences,* 127(2), 621–643. https://doi.org/10.32604/cmes.2021.014407

[5]. Almetwally, E. M., and Ibrahim, G. M. (2020). Discrete alpha power inverse Lomax distribution with application of COVID-19 data. *International Journal of Applied Mathematics,* 9(6), 11–22.

[6]. Al-Marzouki, S., Jamal, F., Chesneau, C., and Elgarhy, M. (2021). Half logistic inverse Lomax distribution with applications. *Symmetry,* 13(2), 309. https://doi.org/10.3390/sym13020309

[7]. Alzaatreh, A., Lee, C., and Famoye, F. (2013). A new method for generating families of continuous distributions. *Metron,* 71(1), 63–79. https://doi.org/10.1007/s40300-013-0007-y

[8]. Alyami, S. A., Elbatal, I., Hassan, A. S., and Almetwally, E. M. (2023). Engineering applications with stress–strength for a new flexible extension of inverse Lomax model: Bayesian and non-Bayesian inference. *Axioms,* 12(12), 1097. https://doi.org/10.3390/axioms12121097

[9]. Atkinson, A., and Harrison, A. (1978). *Distribution of personal wealth in Britain*. Cambridge University Press.

[10]. Bashiru, S. O., and Itopa, I. I. (2023). Modelling of reliability and survival data with exponentiated generalized inverse Lomax distribution. *Reliability: Theory and Applications,* 18(4), 493–501.

[11]. Bowley, A. L. (1926). *Elements of statistics*. King.

[12]. Corbellini, A., Crosato, L., Ganugi, P., and Mazzoli, M. (2010). Fitting Pareto II distributions on firm size: Statistical methodology and economic puzzles. In C. Skiadas (Ed.), *Advances in data analysis, statistics for industry and technology* (pp. 321–328). Birkhäuser. https://doi.org/10.1007/978-0-8176-4799-5_26

[13]. Ehizojie, E. E. (2026). A new flexible generalized distribution: The modified Kies inverse Weibull distribution with properties, estimations and applications. *Journal of Science and Technology*, 18(1), 155–186. https://doi.org/10.30880/jst.2026.18.01.014

[14]. Ghitany, M. E., Al-Mutari, D. K., Balakrishnan, N., and Al-Enezi, L. J. (2013). Power Lindley distribution and associated inference. *Computational Statistics and Data Analysis,* 64, 20–33. https://doi.org/10.1016/j.csda.2013.02.003

[15]. Hadi, H. H., Hilal, O. A., and Al-Noor, N. H. (2025). Extended inverse Lomax distribution with simulation and application to crude birth rate data. *Al-Nahrain Journal of Science,* 28(1), 45–58. https://doi.org/10.22401/ANJS.28.1.06

[16]. Harris, C. M. (1968). The Pareto distribution as a queue service discipline. *Operations Research,* 16(2), 307–313. https://doi.org/10.1287/opre.16.2.307

[17]. Hassan, A. S., and Al-Ghamdi, A. (2009). Optimum step stress accelerated life testing for Lomax distribution. *Journal of Applied Sciences Research,* 5(12), 2153–2164.
[18]. Hassan, A. S., Al-Omar, A. I., Ismail, D. M., and Al-Anzi, A. (2021). A new generalization of the inverse Lomax distribution with statistical properties and applications. *International Journal of Advanced and Applied Sciences*, 8(4), 89–97.
[19]. Hassan, A. S., Assar, S. M., and Shelbaia, A. (2016). Optimum step-stress accelerated life test plan for Lomax distribution with an adaptive type-II progressive hybrid censoring. *Journal of Advances in Mathematics and Computer Science,* 13(2), 1–19. https://doi.org/10.9734/BJMCS/2016/21964
[20]. Hassan, A. S., and Mohamed, R. E. (2019). Weibull inverse Lomax distribution. *Pakistan Journal of Statistics and Operation Research,* 15(3), 587–603. https://doi.org/10.18187/pjsor.v15i3.2378
[21]. Holland, O., Golaup, A., and Aghvami, A. H. (2006). Traffic characteristics of aggregated module downloads for mobile terminal reconfiguration. *IEE Proceedings – Communications,* 153(5), 683–690. https://doi.org/10.1049/ip-com:20045155
[22]. Kleiber, C., and Kotz, S. (2003). *Statistical size distributions in economics and actuarial sciences*. Wiley. https://doi.org/10.1002/0471457175
[23]. Lomax, K. S. (1954). Business failures: Another example of the analysis of failure data. *Journal of the American Statistical Association,* 49(268), 847–852. https://doi.org/10.1080/01621459.1954.10501239
[24]. Maxwell, O., Chukwu, A. U., Oyamakin, O. S., and Khaleel, M. A. (2019). The Marshall-Olkin inverse Lomax distribution with application on cancer stem cell. *Journal of Advances in Mathematics and Computer Science,* 33(4), 1–12.
[25]. Moors, J. J. A. (1988). A quantile alternative for kurtosis. *Journal of the Royal Statistical Society: Series D (The Statistician),* 37(1), 25–32.
[26]. Nicholas, M. D., and Padgett, W. J. (2006). A bootstrap control chart for Weibull percentiles. *Quality and Reliability Engineering International,* 22, 141–151. https://doi.org/10.1002/qre.691
[27]. Ogunde, A. A., Chukwu, A. U., and Oseghale, I. O. (2023). The Kumaraswamy generalized inverse Lomax distribution and applications to reliability and survival data. *Scientific African,* 19, e01483. https://doi.org/10.1016/j.sciaf.2022.e01483
[28]. Rahman, J., Aslam, M., and Ali, S. (2013). Estimation and prediction of inverse Lomax model via Bayesian approach. *Caspian Journal of Applied Sciences Research,* 2(3), 43–56.
[29]. Yadav, A. S., Singh, S. K., and Singh, U. (2016). On hybrid censored inverse Lomax distribution: Application to survival data. *Statistica,* 76(2), 185–203. https://doi.org/10.6092/issn.1973-2201/5993
[30]. Yadav, A. S., Singh, S. K., and Singh, U. (2019). Bayesian estimation of for inverse Lomax distribution under progressive type-II censoring scheme. *International Journal of System Assurance Engineering and Management,* 10(5), 905–917. https://doi.org/10.1007/s13198-019-00820-x
[31]. ZeinEldin, R. A., Ahsan ul Haq, M., Hashmi, S., and Elsehety, M. (2020). Alpha power transformed inverse Lomax distribution with different methods of estimation and applications. *Complexity*, 1860813. https://doi.org/10.1155/2020/1860813

[32]. ZeinEldin, R. A., Ahsan ul Haq, M., Hashmi, S., Elsehety, M., and Elgarhy, M. (2020). Statistical inference of odd Fréchet inverse Lomax distribution with applications. *Complexity,* 4658596. https://doi.org/10.1155/2020/4658596